Journal of Chromatography A, 1218 (2011) 3601–3607

Contents lists available at ScienceDirect

Journal of Chromatography A

journal homepage: www.elsevier.com/locate/chroma

Polydopamine supported preparation method for solid-phase microextraction coatings on stainless steel wire

Juanjuan Feng[a,b], Min Sun[a,b], Jubai Li[a], Lili Xu[a,b], Xia Liu[a], Shengxiang Jiang[a,*]

[a] Key Laboratory of Chemistry of Northwestern Plant Resources, CAS/Key Laboratory for Natural Medicine of Gansu Province, Lanzhou Institute of Chemical Physics, Chinese Academy of Sciences, No. 18 Tianshui Road, Lanzhou, Gansu 730000, China
[b] Graduate University of Chinese Academy of Sciences, Beijing 100039, China

ARTICLE INFO

Article history:
Received 11 January 2011
Received in revised form 4 April 2011
Accepted 6 April 2011
Available online 14 April 2011

Keywords:
Solid-phase microextraction
Polydopamine
Hydroxyapatite
Polycyclic aromatic hydrocarbons
Stainless steel wire

ABSTRACT

In this paper, we introduced a novel and versatile route to prepare solid-phase microextraction coatings on the chemically inert stainless steel wire. Polydopamine films can be created on metallic substrates by an oxidant-induced polymerization and subsequently support various secondary reactions to prepare functional surfaces. In the present work, polydopamine-bioactivated stainless steel wire was successfully modified by nanostructured hydroxyapatite. Extraction performance of the fiber was assessed on several polycyclic aromatic hydrocarbons in water solutions. Extraction mechanism was suggested based on the correlation of partition coefficients and Log Ps. Both aqueous and solid real life samples were used to test the reliability of the solid-phase microextraction-gas chromatography method; some analytes were detected and quantified.

1. Introduction

Solid-phase microextraction (SPME), firstly introduced in 1990s [1], has got considerable developments and wide analytical applications because of its combination of sampling, preconcentration, matrix removal and sample introduction steps [2]. All kinds of organic and inorganic materials [3–6] have been used as coating absorbents to improve the extraction performance of SPME. Moreover, to overcome the fragile drawback of the fused-silica fiber, metal wires become promising support substrates for SPME [2,7–11].

However, because of the chemically inert property, modification of the metal wire is difficult and complicated, which brings much limitation for its application. In recent years, some special processes have been introduced to prepare metal-based SPME fibers. Mehdinia and colleagues [7] prepared a nanostructured lead dioxide SPME fiber via electrochemical deposition on a platinum wire. Djozan [8] used an anodized aluminum wire for the extraction of some aromatic hydrocarbons from gaseous samples. Cao [9] fabricated a nanostructured titania-based SPME fiber through the in situ oxidation of titanium wires with H_2O_2. Yan's group [10] etched the stainless steel wire with hydrofluoric acid and a flower-like structure with Fe_2O_3, FeF_3, Cr_2O_3 and CrF_2 on the surface of the metal wire was produced. Most of the methods mentioned above were innovative and practical, but cannot be applied to many other absorbents because of their selectivity and specificity towards the support and absorbent materials. Minet and colleagues [2] used 11-(2-bromoisobutyrate)-undecyl-1-phosphonic acid to functionalize the stainless steel wire and to initiate the atom transfer radical polymerization. Based on this universal method, a lot of different homopolymers, statistical or block copolymers, undoped or doped with nanoparticles can be obtained as SPME coatings.

In 2007, Messersmith and co-workers [12] drew inspiration from the adhesive proteins created by mussels and found that dopamine and other catechol compounds perform well as binding agents for coating various substrates via covalent and noncovalent interactions. The robust dopamine-derived films (polydopamine) contains catechol and quinine functional groups, and can subsequently support a variety of secondary reactions to create a wide range of functional surfaces [13]. Fan et al. [14] used it as initiator for the surface-initiated polymerization of poly(ethylene glycol) on Ti and stainless steel. Xu [15] used dopamine as the stable anchor to prepare functional molecules on the surface of iron oxide nanoparticles. Ou [16] fabricated uniform TiO_2 films on different polymer substrates by polydopamine-assisted liquid phase deposition process. The versatility of the polydopamine films reflects not only the wide variety of surfaces coated but also the variety of possible treatments [13]. So preparation of SPME coatings on stainless steel wire can be developed via polydopamine derivation with organic or inorganic absorbent materials.

Hydroxyapatite (HAP), as a promising material, has got considerable applications in analytical chemistry because of its

* Corresponding author. Tel.: +86 931 4968266; fax: +86 931 8277088.
E-mail address: sxjiang@lzb.ac.cn (S. Jiang).

0021-9673/$ – see front matter © 2011 Elsevier B.V. All rights reserved.
doi:10.1016/j.chroma.2011.04.018

adsorptivity, biocompatibility and manifold interaction modes. It has been used as stationary phase in high-performance liquid chromatography [17–19], solid-phase extraction [20] and electrochemical sensing to heavy metals [21]. In this paper, we prepared a novel SPME fiber with nanostructured hydroxyapatite (NHAP) as the coating, by a process of polydopamine-assisted biomineralization [22]. Surface properties of the fiber were characterized by field emission scanning electron microscopy (FESEM) and X-ray photoelectron spectroscope (XPS) and the extraction performance was carried out on several polycyclic aromatic hydrocarbons (PAHs). According to the distribution of PAHs in environment, real samples with aqueous and solid matrix were used to test the reliability of the established SPME–GC method.

2. Experimental

2.1. Reagents and chemicals

Dopamine hydrochloride was obtained from Shanghai Experiment reagent Co. (Shanghai, China); tris-(hydroxymethyl) aminomethane (Tirs) was obtained from Shanghai Chemical Plant (Shanghai, China); sodium phosphate dibasic dodecahydrate ($Na_2HPO_4{\cdot}12H_2O$) and sodium chloride (NaCl) were purchased from Beijing Shuanghuan WeiYe reagent Co. (Beijing, China); magnesium chloride hexahydrate ($MgCl_2{\cdot}6H_2O$), potassium chloride (KCl), and sodium sulfate anhydrous (Na_2SO_4) were purchased from Shanghai Shanpu Chemical Industry (Shanghai, China); sodium bicarbonate ($NaHCO_3$) and calcium chloride hexahydrate ($CaCl_2{\cdot}6H_2O$) were obtained from Tianjin Chemical Reagent Plant 1. (Tianjin, China). Fluorene (Flu), fluoranthene (Flt), anthracene (Ant), benzo(a)anthracene (BaA), chrysene (Chr) and benzo(a)pyrene (BaP) were obtained from the Shanghai Chemical Reagent Factory (Shanghai, China). All chemicals were used directly without any treatment.

2.2. Apparatus

Analysis of the model compounds was performed with an Agilent 7890 GC system (Agilent Technologies, USA) equipped with a flame ionic detector (FID) and a split/splitless injector. The column used for the separation was SE-54 capillary column (30 m × 0.32 mm id × 0.33 μm film thickness).

Ultrapure nitrogen (>99.999%) was used as the carrier and make-up gas at 1 mL min^{-1} and 45 mL min^{-1}, respectively. Both the injector and detector temperatures were fixed at 300 °C. Separation was achieved using temperature programs as follows: the column temperature was initially held at 100 °C, and programmed at 30 °C min^{-1} to 280 °C, being hold for 5.3 min, then at the rate of 40 °C min^{-1} to 300 °C, then being hold for 5 min.

Surface characteristics of the NHAP/SPME fiber were obtained on a field emission scanning electron microscope (FESEM, JSM-6701F, Japan).

An X-ray photoelectron spectroscope (XPS, Escalab 210, VG Scientific, UK) was applied to certify the existence of the NHAP on the fiber.

2.3. Preparation of sample solutions

All the analytes (Flu, Flt, Ant, BaA, Chr and BaP) were dissolved in ethanol with concentration at 0.2 mg mL^{-1} as stored solution and kept at 4 °C for use.

On basis of the distribution of PAHs in environment, real samples with aqueous (water from Yellow River and local waterworks) and solid (sediment from Yellow River and soil from chemical industrial park) matrix were chosen to test the reliability of the proposed method. Aqueous samples were filtered through 0.45 μm membrane and stored at 4 °C. The preparation of the soild samples was adapted from previous reports [23,24]. In detail, 2.0 g solid sample was extracted by a 10 mL aliquot of hexane/dichloromethane (1:1, v/v) with ultrasonic agitation for 15 min. Suspensions were separated by centrifugation at 4500 rpm and then another fresh 10 mL aliquot organic solvent was used to extract for another 15 min. The combined extracts were reduced to approximately 5 mL with a vacuum rotary evaporator at 35 °C and then evaporated to almost dryness under a gentle stream of nitrogen. The residue was reconstituted with 100 μL ethanol and 10 mL water. The solution was stored at 4 °C for SPME extraction.

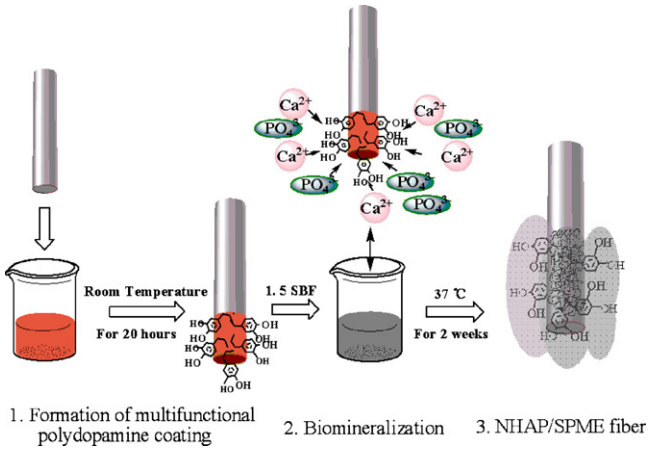

Fig. 1. Schema of preparation procedures of the fiber.

2.4. Preparation of SPME fiber

One end of the stainless steel wire with length about 2.5 cm was washed before use with acetone, ethanol and distilled water in an ultrasonic bath for 5 min respectively. The biomineralization routes of the wire were derived from the previous report [22] and indicated in Fig. 1. Briefly, 20 mg of dopamine–hydrochloride was dissolved in 10 mL of 10 mmol L^{-1} Tris buffer and the final pH was adjusted to 8.5. The treated end of the stainless steel wire was immersed in the dopamine–Tris buffer solution for 20 h at room temperature. A thin layer of polydopamine was coated on the surface of the wire. Then the wire was rinsed with deionized water thoroughly and dried with a stream of N_2 gas. Afterwards, the stainless steel wire was transferred into 1.5× simulated body fluid (SBF) and kept at 37 °C to grow NHAP for about 2 weeks. Finally, the fiber was taken out, rinsed with deionized water and dried at room temperature. 1.5× SBF contained Na^+, 213.0; K^+, 7.5; Mg^{2+}, 2.25; Ca^{2+}, 3.75; Cl^-, 221.7; HCO_3^-, 6.3; HPO_4^{2-}, 1.5; SO_4^{2-}, 0.75 mmol L^{-1}.

2.5. Solid-phase microextraction

The fiber was equipped into a homemade SPME device which was a modification of a 5 μL syringe. All of the fibers were aged in the GC inlet at 300 °C for about 30 min under N_2 flow before use to remove the interferences and stabilize the coating. All SPME extractions were conducted in direct immersion mode with 10 mL working solution in a 15 mL via. A magnetic bar was inside the vial to accelerate the extraction and the stirring rate was fixed at 1000 rpm. After the extraction, the fiber was withdrawn into the needle and subsequently introduced into the GC inlet for thermal desorption and analysis. All the SPME experiments were carried out in triplicate to ensure the accuracy of data.

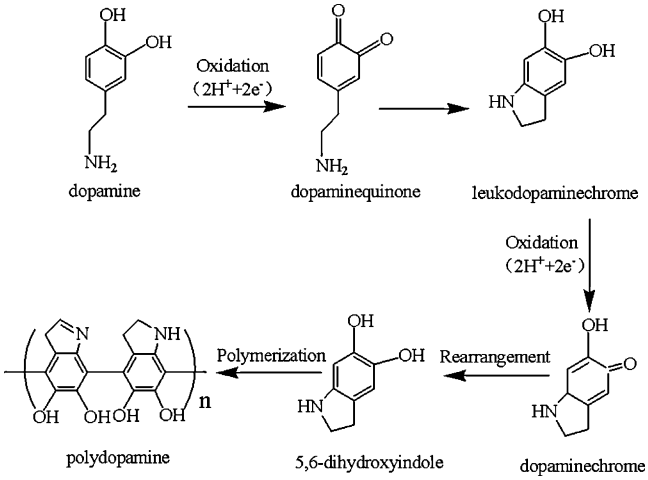

Fig. 2. Multifunctional coating formation by oxidant-induced dopamine polymerization [12,25].

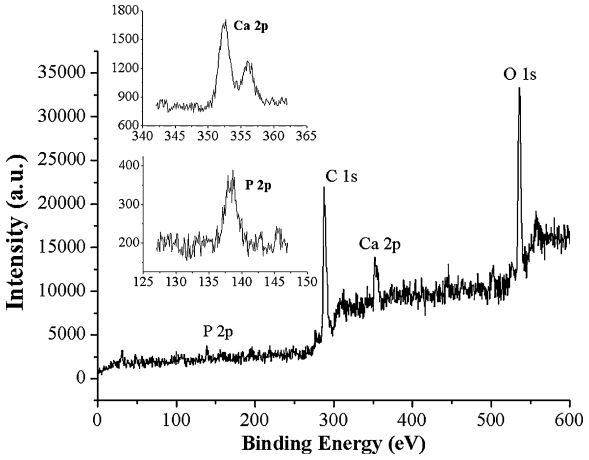

Fig. 4. XPS images of the fiber.

3. Results and discussion

3.1. Preparation of the fiber

Dopamine spontaneously polymerizes at alkaline condition (pH = 8.5) to form a robust polydopamine coating, which exhibits latent reactivity because of the existence of the catechol and quinine functional groups (as shown in Fig. 2). In the present work, polydopamine acted as binding agent and assisted the formation of NHAP onto the wire surface at the same time. It took about 2 weeks time to cover the substrate fully and uniformly. As shown in Fig. 3, a typically lath-like form of NHAP crystals is obtained. The unit of the lath is very fine, and this brings large surface area to the fiber, which is favorable for high extraction capability. Under the influence of preparation conditions [26], the Ca/P ratio from energy dispersive spectrometer (EDS) is 1.62, close to the stoichiometric ratio of 1.67.

Surface analysis by XPS demonstrates the formation of NHAP. As shown in Fig. 4, the fiber exhibits O 1s, Ca 2p, C 1s and P 2p peaks at 536, 353, 293 and 138 eV, respectively. There is no substrate peak of Fe, Mn, Ni, or Cr. So the stainless steel wire has been fully coated by NHAP.

3.2. Optimization of SPME parameters

3.2.1. Extraction parameters

To obtain the highest extraction efficiency, extraction parameters were optimized, including extraction temperature, extraction time, ionic strength and pH. The working solution (0.1 μg mL^{-1}, 10 mL) in a 15 mL vial was prepared by diluting the stored solution with distilled water.

Based on the investigations (Figs. 5–7), extraction at 50 °C for about 30 min with KCl concentration at 20 wt.% were fixed as the optimum extraction conditions. Besides, from the extraction analysis of the fiber in Section 3.5, a cation-π interaction between the positively charged Ca^{2+} on HAP [27] and the electron-rich π-system

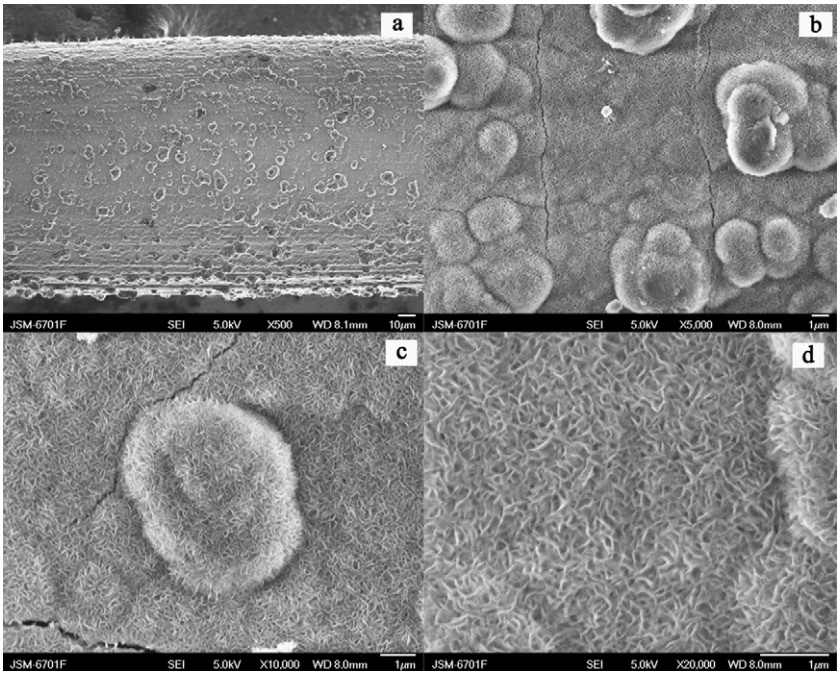

Fig. 3. FESEM images of the fiber with magnification at 500 (a); 5000 (b); 10,000 (c) and 20,000 (d).

Table 1
Analytical parameters of the established SPME–GC-FID method for the determination of PAHs and LODs of other SPME fibers coupled to GC-FID.

Compound	Linear range ($\mu g\,L^{-1}$)	Linearity (R^2)	LOD ($ng\,L^{-1}$)	Repeatability ($n=5$, %, single fiber)	Reproducibility ($n=3$, %, fiber-to-fiber)	LODs of commercial PDMS fiber (100 μm) [30] ($ng\,L^{-1}$)	LODs of commercial PA fiber (85 μm) [30] ($ng\,L^{-1}$)	LODs of PPy-DS fiber [31] ($ng\,L^{-1}$)	LODs of etched stainless steel wire [10] ($ng\,L^{-1}$)	LODs of TiO_2 nanotube array/Ti wire [32] ($ng\,L^{-1}$)
Flu	0.5–200	0.9933	40	6.0	10.6	80	80	50	300	100
Ant	0.2–200	0.9842	40	7.7	8.1	180	110	–	–	10
Flt	0.2–200	0.9981	40	4.7	15.8	250	170	120	580	10
BaA	0.1–200	0.9919	20	7.9	13.9	290	50	–	–	–
Chr	0.1–200	0.9865	20	13.0	15.1	240	160	150	–	–
BaP	0.1–200	0.9994	20	8.1	12.8	440	160	–	–	–

Conditions: extraction time, 30 min; extraction temperature, 50 °C; pH = 6.5; content of KCl, 20 wt.%; desorption time, 5 min; desorption temperature, 300 °C.

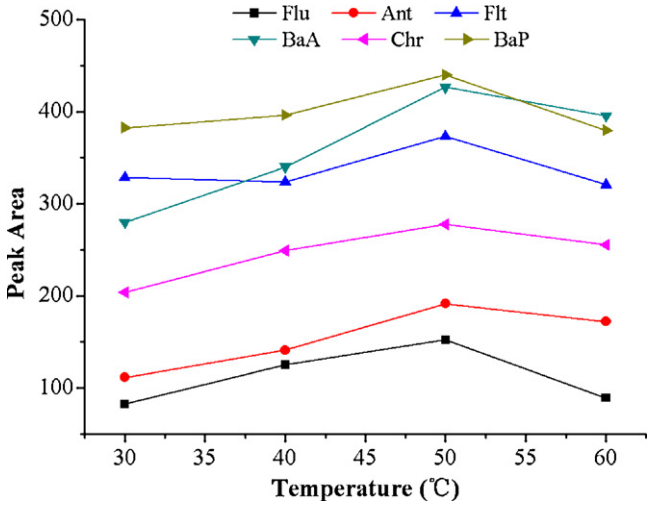

Fig. 5. Effect of temperature on peak area. Conditions: analytes concentration, 0.1 $\mu g\,mL^{-1}$; extraction time, 30 min; content of KCl, 20 wt.%; pH = 6.5; desorption time, 5 min; desorption temperature, 300 °C.

of analytes may be involved in the extraction mechanism [28]. HAP is positively charged under low pH condition (pH < 9) [20]. But it is acid nonresistant material; solubility of HAP occurs at pH values below 6.5 [29]. So 6.5 was chosen as the final pH value of the working solution.

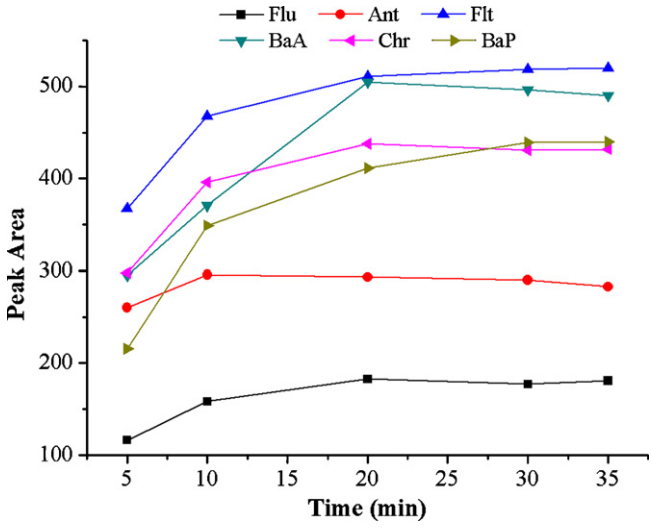

Fig. 6. Effect of extraction time on peak area. Conditions: analytes concentration, 0.1 $\mu g\,mL^{-1}$; extraction temperature, 50 °C; content of KCl, 20 wt.%; pH = 6.5; desorption time, 5 min; desorption temperature, 300 °C.

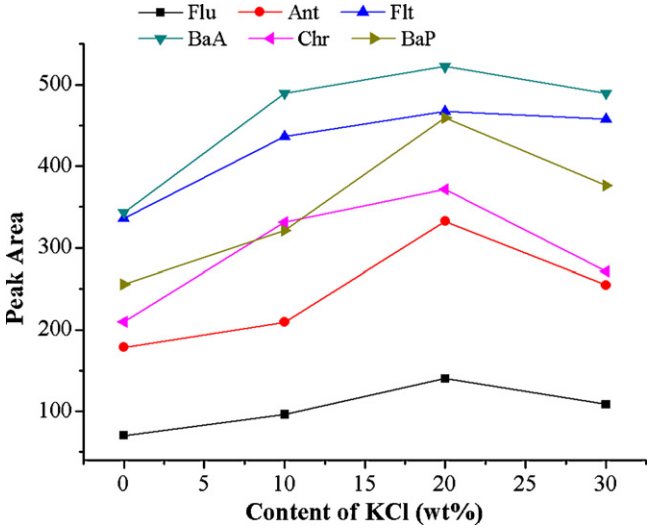

Fig. 7. Effect of content of KCl on peak area. Conditions: analytes concentrations, 0.1 $\mu g\,mL^{-1}$; extraction time, 30 min; extraction temperature, 50 °C; pH = 6.5; desorption time, 5 min; desorption temperature, 300 °C.

3.2.2. Desorption parameters

The fiber was desorbed at different temperatures, ranging from 280 to 320 °C, to obtain complete desorption of the analytes. Because of the high boiling points of the analytes, 300 °C was satisfactory for the complete desorption. The desorption time was studied from 2 to 6 min. As can be seen in Fig. 8, the highest peak area was reached at 5 min. Test for carry-over effects of the system was also done by a second desorption of the fiber. No peaks were observed at the retention time of the analytes. So desorption at 300 °C for 5 min was used for the SPME procedure.

3.3. Analytical parameters

The analytical data of the established SPME–GC method such as linear range, correlation of the calibration (R^2), limit of detection (LOD), repeatability (RSD) for single fiber and fiber-to-fiber reproducibility were measured under the optimized conditions and summarized in Table 1.

The linearity of the method was tested by preparing an analytical curve for each analytes with increasing concentration from 5 $ng\,L^{-1}$ to 500 $\mu g\,L^{-1}$. Calibration curves were constructed by plotting peak areas verse the concentration of the analytes ($\mu g\,L^{-1}$). The SPME procedure showed a wide linear range with correlation coefficients (R^2) varying from 0.9842 to 0.9994, which indicates the excellent performance of the fiber. The LODs are 40 $ng\,L^{-1}$ for Flu, Ant and Flt and 20 $ng\,L^{-1}$ for BaA, Chr and BaP. A good precision for

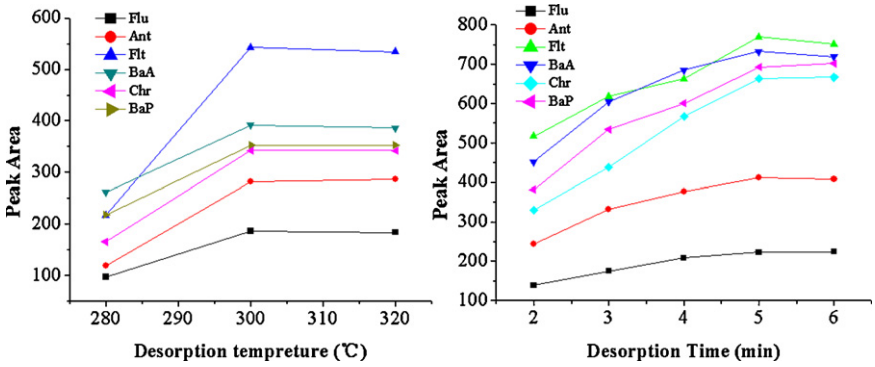

Fig. 8. (a) Effect of desorption temperature. Conditions: analytes concentration, 0.1 μg mL^{-1}; extraction time, 30 min; extraction temperature, 50 °C; pH = 6.5, desorption time, 5 min. (b) Effect of desorption time. Conditions: analytes concentration, 0.1 μg mL^{-1}; extraction time, 30 min; extraction temperature, 50 °C; pH = 6.5, desorption temperature, 300 °C.

analysis of PAHs using single fiber was also obtained, and the RSDs are from 4.7 to 13.0%. The fiber-to-fiber reproducibility was investigated using three different fibers, and the RSDs range from 8.1 to 15.8%. The data show that the preparation method for the fiber is quite stable and acceptable. LODs of proposed SPME fiber were also compared with those of commercial fibers [30] and several novel SPME fibers reported previously [31,10,32] with the same direct immersion mode coupled to GC-FID. It is worth noticing that LODs in this work are much lower than those of PDMS and PA fibers. At the same time, LODs of the established method was comparable with, or even lower than those of the novel fibers listed in Table 1 towards the same analytes. All these showed the good extraction performance of the proposed fiber.

3.4. Stability of the fiber

The coating's lifetime is very important for the practical application of SPME fiber. It is usually damaged by exposure to high temperature, organic solvent, strong acidic and basic solutions [33]. Stability of the fiber was tested by treating it with harsh conditions. As shown in Fig. 9, the fiber shows very well endurance to organic solvent, high temperature and alkali, but it is easily damaged by acid solution. This can be ascribed to the acid nonresistance of HAP. HCl solution dissolved the NHAP coating and the extraction capability was decreased. So pH of the working solution in present work was adjusted to 6.5 to avoid HAP dissolution and obtain the highest extraction capability.

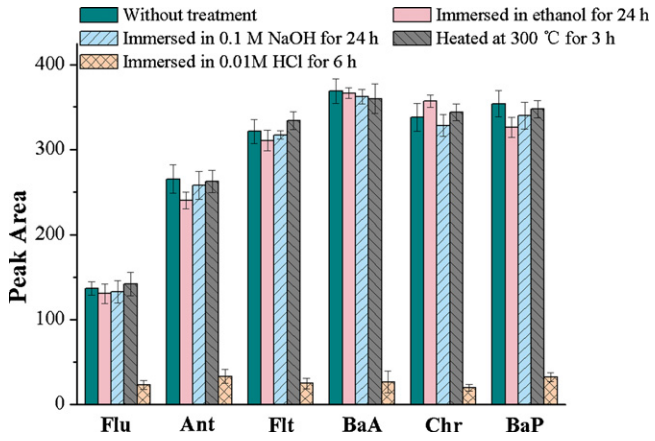

Fig. 9. Stability of the fiber to organic solvent, acid, alkali and high temperature conditions.

3.5. Estimation of partition coefficients and extraction mechanism

Partition coefficient is an important parameter for understanding the sorption mechanism of SPME absorbent as well as for quantitatively determining the extracted amount of analytes [34]. To fully understand the dependence of the extraction efficiency on the analytes' properties and the extraction mechanism of the fiber, partition coefficients (K_{fs}) of the model compounds between the coating material and the aqueous solution were estimated and correlated with their octanol/water partition coefficients (Log P, measurement of how hydrophobic a chemical substance is). Because the extractions are preformed under the equilibrium system, the amounts of analytes partitioned to the coating are proportional to their concentrations in the working solution phase. The partition coefficient can be calculated according to Eq. (1) [35,36].

$$K_{fs} = \frac{V_s}{V_f(n_0/n_f - 1)} \quad (1)$$

where n_0 is the initial amount of analyte in the sample solution, n_f is the amount of analyte on the fiber after equilibrium, V_s is the sample volume, and V_f is the fiber coating volume. In this work, the sample volume (V_s) was 10 mL; the initial amount of analytes (n_0) in the vial was 1 μg; the n_f values, corresponding to the n_0 values selected, were calculated by the calibrations curves (Peak area-Mass) constructed by standard solution. The thickness of the NHAP coating (δ) was 12.25 ± 2.50 μm, which was obtained by the dimension of the SEM images; length of the NHAP coating was 2.5 cm. Volume of the fiber coating (V_f) was calculated as 0.176 μL.

If the volume of the vial is sufficiently large, the concentration change of the solute in the vial before and after SPME is negligible [37]. So the Eq. (1) can be changed as:

$$K_{fs} = \frac{V_s n_f}{V_f n_0} \quad (2)$$

Because of the approximation of the V_f and n_f values, the partition coefficients were only approximate.

The Log K_{fs} values are listed in Table 2 and the correlation of Log K_{fs} and Log P is shown in Fig. 10. A sketchy consistent relationship between Log K_{fs} and Log P is obtained in this work. Hydrophobicity of the analytes contributed to the extraction because of the decrease of solubility, so the Log K_{fs}s increase with the increase of Log Ps of Flu, Ant and Flt. While for BaA, Chr and BaP, Log K_{fs}s are greatly irrelevant to their Log Ps. It seemed that some other factors may be involved in the extraction of PAHs. Actually, a charge-induced dipole–dipole interaction has been suggested for the sorption of PAHs to inorganic mineral surfaces [28,38]. On the surface of the NHAP coated fiber, Ca^{2+} ions acted as the positively charged sorption domains and interacted with the electron-rich

Table 2
Physical properties and the partition coefficients of the analytes.

Compound	Chemical structure	Molecular weight	[a]Log K_{fs}	[b]Log P
Flu		166	3.03	4.18
Ant		178	3.16	4.45
Flt		202	3.38	5.16
BaA		228	3.35	5.76
Chr		228	3.33	5.81
BaP		252	3.38	6.13

[a] Concentration of working solution was 0.1 μg mL^{-1}; extraction and desorption conditions was the same as shown in Table 1.
[b] ChemIDplus Database.

analytes based on the cation-π interaction. Besides, the effect of molecular volume on diffusion may be another factor influencing the extraction efficiency. The increasing molar volume decreased the diffusion coefficient, which was unfavorable for the transference of the analytes from the aqueous phase to the coating. Furthermore, Schlautman and Morgan [39] indicated that the presence of Ca^{2+} at the surface somehow altered the structure of the interfacial water in such a way as to make the surface more hospitable for hydrophobic solutes. So that may be one of the other reasons for the high extraction efficiency of PAHs on the NHAP based fiber.

Nevertheless, because of the small amount of K_{fs} data in present work, correlation between the Log K_{fs} and Log P was only a mere observation.

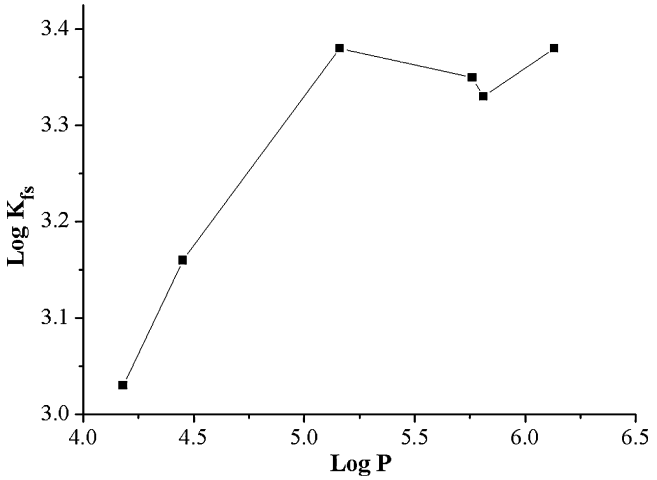

Fig. 10. Correlation of Log K_{fs} and Log P.

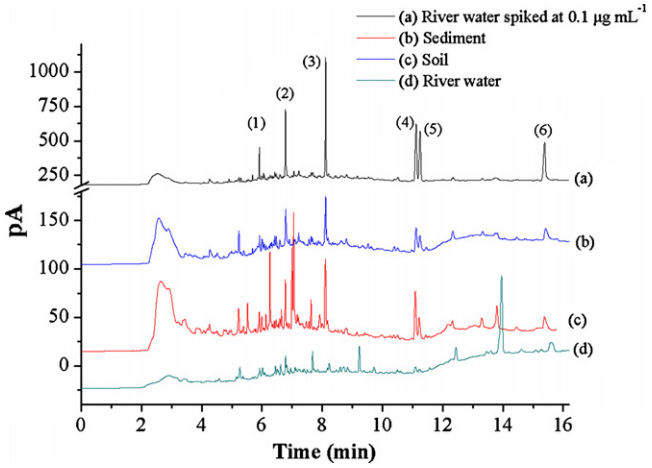

Fig. 11. GC-FID chromatograms of spiked and non-spiked real samples. (1) Flu, (2) Ant, (3) Flt, (4) BaA, (5) Chr and (6) BaP.

3.6. Application to real samples

Arising from both natural and anthropogenic sources, PAHs are ubiquitous in the environment [40,41]. Especially in Western China, the carcinogenous PAHs pollution was serious enough to threaten the public health, which was aroused by historical reasons. According to the distribution of PAHs in environmental matrix, two aqueous samples (collected from Yellow River and local waterworks) and two solid samples (sediment from Yellow River and soil from chemical industrial park) were chosen to investigate the reliability of the NHAP/SPME fiber–GC-FID method for the analysis of environmental samples.

3.6.1. Matrix effect

Matrix effects on recoveries of the target compounds were investigated by extracting fortified samples of river water, running water, and extract solutions of two solid samples under optimum extraction conditions with addition level at 0.1 μg mL^{-1}. The signals of the analytes were corrected by the corresponding signals obtained from non-spiked samples. As can be seen in Table 3, all the real samples provide acceptable recoveries and standard deviations. Recoveries in two solid extract solutions vary more widely from 74.8 to 130.2% with larger standard deviations than that of the two aqueous samples from 77.4 to 113.6%. Fig. 11 is the chromatogram of the non-spiked and spiked real samples. The GC-FID resolution and peak shapes are similar, and that indicate the good purification effect of the proposed fiber, with the joint effect of the ultrasonic extraction.

3.6.2. Determination of PAHs in real samples

Based on the investigation of matrix effects on recoveries, two aqueous samples were determined by external standard calibration curves in Section 3.3. For the accurate quantification of the two solid samples, a standard addition method was employed to compensate the matrix effect with samples spiked at 0.05, 0.10, 0.20, 0.30, 0.40 and 0.50 μg g^{-1}. Taking into account of the losses of PAHs during the preparation process, these spiked samples were exposed to the same protocol (ultrasonic extraction, evaporation and reconstitution steps) [42].

As can be seen in Table 4, all the analytes except Flt and BaP are detected but cannot be quantified in river water. None of the analytes is detected in running waters. Most of the analytes are quantified in two solid samples at high concentration levels, which demonstrate the strong accumulation effect of solid particles to PAHs. Flu, Ant and BaA in soil are quantified to 4.83, 5.14

Table 3
Results of recoveries of the fortified samples spiked with 6 PAHs.

Compound	Added ($\mu g\,mL^{-1}$)	River water		Running water		Sediment		Soil	
		[a]Found ($\mu g\,mL^{-1}$)	[b]Recovery (%)	Found ($\mu g\,mL^{-1}$)	Recovery (%)	Found ($\mu g\,mL^{-1}$)	Recovery (%)	Found ($\mu g\,mL^{-1}$)	Recovery (%)
Flu	0.10	0.095	95.3 ± 4.8	0.103	103.1 ± 3.3	0.125	125.4 ± 1.1	0.124	123.9 ± 6.8
Ant	0.10	0.099	99.3 ± 3.4	0.084	84.4 ± 3.7	0.130	130.2 ± 7.4	0.118	118.0 ± 9.4
Flt	0.10	0.088	88.3 ± 7.1	0.113	112.6 ± 2.3	0.121	121.0 ± 2.1	0.117	117.0 ± 5.5
BaA	0.10	0.107	106.5 ± 2.2	0.095	95.3 ± 9.6	0.089	88.9 ± 10.2	0.108	107.6 ± 4.2
Chr	0.10	0.077	77.4 ± 3.9	0.086	86.2 ± 7.6	0.127	127.0 ± 8.4	0.124	124.1 ± 2.0
BaP	0.10	0.114	113.6 ± 1.5	0.101	101.0 ± 10.0	0.115	115.2 ± 3.0	0.075	74.8 ± 7.0

Conditions: the same as shown in Table 1.
[a] $n = 3$.
[b] Average value ± standard deviation, signals was corrected by corresponding signals from non-spiked samples.

Table 4
Determination results of 6 PAHs in real samples.

Compound	River water ($\mu g\,L^{-1}$)	Running water ($\mu g\,L^{-1}$)	Sediment		Soil	
			[a]Calibration curve	[b]Concentration ($ng\,g^{-1}$)	Calibration curve	Concentration ($ng\,g^{-1}$)
Flu	Not quantified	Not detected	$Y = 18.85X + 5.74$	Not quantified	$Y = 2.39X + 11.54$	4.83
Ant	Not quantified	Not detected	$Y = 18.59X + 37.31$	2.01	$Y = 8.59X + 44.15$	5.14
Flt	Not detected	Not detected	$Y = 15.54X + 27.54$	1.77	$Y = 21.07X + 49.10$	2.33
BaA	Not quantified	Not detected	$Y = 12.54X + 27.77$	2.22	$Y = 13.18X + 49.34$	3.74
Chr	Not quantified	Not detected	$Y = 15.04X + 16.62$	1.10	$Y = 10.67X + 25.62$	2.40
BaP	Not detected	Not detected	$Y = 19.60X + 50.53$	2.58	$Y = 14.64X + 30.89$	2.11
Total ($\mu g\,L^{-1}$/$ng\,g^{-1}$)	–	–	–	9.68	–	20.55

Conditions: the same as shown in Table 1.
[a] From the standard addition method.
[b] Concentrations of model PAHs in soil samples.

and 3.74 $ng\,g^{-1}$, respectively. Concentration of BaP in sediment is detected at 2.58 $ng\,g^{-1}$. Total amount of the model PAHs in two solid samples is 9.68 and 20.55 $ng\,g^{-1}$, respectively.

4. Conclusion

A novel NHAP/SPME fiber was prepared by a simple polydopamine-assisted biomineralization process. Extraction performance was evaluated by extracting several PAHs in aqueous samples. Analytical parameters were all investigated, which demonstrated the fine extraction capabilities of the fiber. According to the distribution of PAHs in environment matrix, both aqueous and solid samples were used to test the reliability of the SPME–GC method.

Partition coefficients of the analytes between the coating and the aqueous solution were estimated and correlated with their Log Ps. Extraction mechanism was suggested based on the experimental results and some related references, which predicted its potential extraction capability to other compounds with large π-electron system.

Due to the fine compatibility with metal substrates and the multifunctional property for surface modification, polydopamine has sparked great interest as binding agent in the preparation of SPME fiber with metal wire as support.

Acknowledgment

This work was supported by the National Natural Science Foundation of China (Nos. 20975105, 20775084, 20805052).

References

[1] R.P. Belardi, J. Pawliszyn, Water Pollut. Res. J. Can. 24 (1989) 179.
[2] I. Minet, L. Hevesi, M. Azenha, J. Delhalle, Z. Mekhalif, J. Chromatogr. A 1217 (2010) 2758.
[3] A.K. Malik, V. Kaur, N. Verma, Talanta 68 (2006) 842.
[4] X.G. Hu, J.L. Pan, Y.L. Hu, Y. Huo, G.K. Li, J. Chromatogr. A 1188 (2008) 97.
[5] J.C. Wu, J. Pawliszyn, Anal. Chim. Acta 520 (2004) 257.
[6] J.W. Zewe, J.K. Steach, S.V. Olesik, Anal. Chem. 82 (2010) 5341.
[7] A. Mehdinia, M.F. Mousavi, M. Shamsipur, J. Chromatogr. A 1134 (2006) 24.
[8] D. Djozan, Y. Assadi, S.H. Haddadi, Anal. Chem. 73 (2001) 4054.
[9] D.D. Cao, J.X. Lü, J.F. Liu, G.B. Jiang, Anal. Chim. Acta 611 (2008) 56.
[10] H.L. Xu, Y. Li, D.Q. Jiang, X.P. Yan, Anal. Chem. 81 (2009) 4971.
[11] J.J. Feng, M. Sun, H.M. Liu, J.B. Li, X. Liu, S.X. Jiang, J. Chromatogr. A 1217 (2010) 8079.
[12] H. Lee, S.M. Dellatore, W.M. Miller, P.B. Messersmith, Science 318 (2007) 426.
[13] J.H. Waite, Nat. Mater. 7 (2008) 8.
[14] X.W. Fan, L.J. Lin, J.L. Dalsin, P.B. Messersmith, J. Am. Chem. Soc. 127 (2005) 15843.
[15] C.J. Xu, K.M. Xu, H.W. Gu, R.K. Zheng, H. Liu, et al., J. Am. Chem. Soc. 126 (2004) 9938.
[16] J.F. Ou, J.Q. Wang, D. Zhang, P.L. Zhang, S. Liu, et al., Colloids Surf. B 76 (2010) 123.
[17] A. Tiselius, S. Hjérten, O. Arch, Biochem. Biophys. 65 (1956) 132.
[18] S.R. Shepard, C. Brickman-Stone, J.L. Schrimsher, G. Koch, J. Chromatogr. A 891 (2000) 93.
[19] T. Li, Y.Q. Feng, Talanta 80 (2009) 889.
[20] S.B. Yu, J. Geng, P. Zhou, J. Wang, X.D. Chen, J.M. Hu, J. Chromatogr. A 1183 (2008) 29.
[21] D.W. Pan, Y.E. Wang, Z.P. Chen, T.T. Lou, W. Qin, Anal. Chem. 81 (2009) 5088.
[22] J. Ryu, S.H. Ku, H. Lee, C.B. Park, Adv. Funct. Mater. 20 (2010) 1.
[23] Y.H. Wang, J. Zhang, Y.C. Ding, J. Zhou, L.X. Ni, C. Su, J. Sep. Sci. 32 (2009) 3951.
[24] N. Ratola, S. Lacorte, A. Alves, D. Barceló, J. Chromatogr. A 1114 (2006) 198.
[25] Q. Wei, F.L. Zhang, J. Li, B.J. Li, C.S. Zhao, Polym. Chem. 1 (2010) 1430.
[26] Z.H. Cheng, A. Yasukawa, K. Kandori, T. Ishikawa, Langmuir 14 (1998) 6681.
[27] K. Kandori, A. Fudo, T. Ishikawa, Colloids Surf. B 24 (2002) 145.
[28] S. Müller, K.U. Totsche, I. Kögel-Knabner, Eur. J. Soil Sci. 58 (2007) 918.
[29] L. Dattolo, E.L. Keller, G. Carta, J. Chromatogr. A 1217 (2010) 7573.
[30] R.A. Doong, S.M. Chang, Y.C. Sun, J. Chromatogr. A 879 (2000) 177.
[31] A. Mohammadi, Y. Yamini, N. Alizadeh, J. Chromatogr. A 1063 (2005) 1.
[32] H.M. Liu, D.A. Wang, L. Ji, J.B. Li, S.J. Liu, X. Liu, S.X. Jiang, J. Chromatogr. A 1217 (2010) 1898.
[33] X.Y. Liu, Y.S. Ji, Y.H. Zhang, H.X. Zhang, M.C. Liu, J. Chromatogr. A 1165 (2007) 10.
[34] R.A. Doong, S.M. Chang, Anal. Chem. 72 (2000) 3647.
[35] J. Pawliszyn, Solid-Phase Microextraction: Theory and Practice, Wiley-VCH, Chichester, 1997.
[36] J. López-Darias, V. Pino, Y.J. Meng, J.L. Anderson, A.M. Afonso, J. Chromatogr. A 1217 (2010) 7189.
[37] R.F. Jiang, F. Zhu, T.G. Luan, Y.X. Tong, H. Liu, G.F. Ouyang, J. Pawliszyn, J. Chromatogr. A 1216 (2009) 4641.
[38] B.T. Mader, K.U. Goss, S.J. Eisenreich, Environ. Sci. Technol. 31 (1997) 1079.
[39] M.A. Schlautman, J.J. Morgan, Environ. Sci. Technol. 28 (1994) 2184.
[40] J.Y. Guo, F.C. Wu, X.J. Luo, Z. Liang, H.Q. Liao, et al., Environ. Pollut. 158 (2010) 2175.
[41] S. Xu, W. Liu, S. Tao, Environ. Sci. Technol. 40 (2006) 702.
[42] J. Sanz-Landaluze, M. Bocanegra-Salazar, D. Ortiz-Pérez, C. Cámara, J. Chromatogr. A 1217 (2010) 3567.